14q32 rearrangements deregulating BCL11B mark a distinct subgroup of T-lymphoid and myeloid immature acute leukemia

14q32 rearrangements deregulating *BCL11B* mark a distinct subgroup of T and myeloid immature acute leukemia

Short title: *BCL11B* activation in immature acute leukemia

Danika Di Giacomo,[1,*] Roberta La Starza,[1,*] Paolo Gorello,[1] Fabrizia Pellanera,[1] Zeynep Kalender Atak,[2,3] Kim De Keersmaecker,[4] Valentina Pierini,[1] Christine J. Harrison,[5] Silvia Arniani,[1] Martina Moretti,[1] Nicoletta Testoni,[6] Giovanna De Santis,[7] Giovanni Roti,[8] Caterina Matteucci,[1] Renato Bassan,[9] Peter Vandenberghe,[10] Stein Aerts,[2] Jan Cools,[11] Beat Bornhauser,[12] Jean Pierre Bourquin,[12] Rocco Piazza,[13] Cristina Mecucci.[1]

[1]Department of Medicine, Center for Hemato-Oncology Research (C.R.E.O.), University of Perugia, Perugia, Italy;
[2]Laboratory of Computational Biology, KU Leuven Center for Human Genetics, Leuven, Belgium;
[3]Current address: Cancer Research UK Cambridge Institute, University of Cambridge, Cambridge UK;
[4]Department of Oncology, KU Leuven and Leuven Cancer Institute, Leuven, Belgium;
[5]Leukaemia Research Cytogenetics Group, Translational and Clinical Research Institute, Newcastle University Centre for Cancer, Newcastle-upon-Tyne, UK;
[6]"Seràgnoli" Institute of Hematology, Department of Experimental, Diagnostic and Specialty Medicine, University of Bologna, Italy;
[7]U.O.C. of Hematology, Regional Hospital, Avellino, Italy;
[8]University of Parma, Department of Medicine and Surgery, Parma, Italy;
[9]U.O.C. of Haematology, dell' Angelo Hospital and Santissimi Giovanni and Paolo Hospital, Mestre and Venice, Italy;
[10]Department of Human Genetics, KU Leuven and Department of Hematology, University Hospitals Leuven, Belgium;
[11]VIB-KU Leuven Center for Cancer Biology and Center for Human Genetics, Leuven, Belgium;
[12]University Children's Hospital, Division of Pediatric Oncology, University of Zurich, Switzerland;
[13]Department of Medicine & Surgery, University of Milano-Bicocca, Italy.

[*] These authors contributed equally to this work

Correspondence Address:
Cristina Mecucci, M.D.,PhD
Hematology, University of Perugia, CREO, P.le Menghini 9, 06132, Perugia, Italy
e-mail: cristina.mecucci@unipg.it
Tel: +39-075-5783808; Fax: +39-075-5783691

Text word count: 3651

Abstract word count: 250

Number of Figures and Tables: 6. Number of supplemental Figures and Tables: 21

Number of References: 52. Number of Supplemental References: 20

Scientific Category: Myeloid Neoplasia; Lymphoid Neoplasia

Key points

14q32 rearrangements, activating *BCL11B,* provide a novel biomarker for a new entity among immature acute leukemia.

Abstract

Acute leukemias (AL) of ambiguous lineage are a heterogeneous group of high-risk leukemias characterized by co-expression of myeloid and lymphoid markers. In this study, we identified a distinct subgroup of immature acute leukemias characterized by a broadly variable phenotype, covering acute myeloid leukemia (AML M0 or M1), T/myeloid mixed phenotype acute leukemia (T/M MPAL), and early T-cell precursor acute lymphoblastic leukemia (ETP-ALL). Rearrangements at 14q32/*BCL11B* are the cytogenetic hallmark of this entity. In our screening of 915 hematological malignancies, there were 202 AML and 333 T-cell Acute Lymphoblastic Leukemia (T-ALL) (58 ETP, 178 non-ETP, 8 T/M MPAL, 89 not otherwise specified). We identified 20 cases of immature leukemias (4% of AML and 3,6% of T-ALL) harbouring four types of 14q32/*BCL11B* translocations: t(2,14)(q22.3;q32) (n=7), t(6;14)(q25.3;q32) (n=9), t(7;14)(q21.2;q32) (n=2) and t(8;14)(q24.2;q32) (n=2). The t(2;14) produced a *ZEB2-BCL11B* fusion transcript, while the other three rearrangements displaced transcriptionally active enhancer sequences close to *BCL11B* without producing fusion genes. All translocations resulted in the activation of *BCL11B,* a regulator of T-cell differentiation associated with transcriptional corepressor complexes in mammalian cells. The expression of *BCL11B* behaved as a disease biomarker, which was present at diagnosis but not in remission.

Deregulation of *BCL11B* co-occurred with variants at *FLT3* and at epigenetic modulators, most frequently *DNMT3A*, *TET2* and/or *WT1* gene. Transcriptome analysis identified a specific expression signature, with significant downregulation of BCL11B targets, and clearly separating *BCL11B* positive AL from AML, T-ALL, and ETP-ALL. Remarkably, ex-vivo drug sensitivity profile identified a panel of compounds with effective antileukemic activity.

Keywords

Immature acute myeloid leukemia; T-ALL; ETP-ALL; T/M MPAL; *BCL11B* activation; 14q32 rearrangements; expression profile; drug sensitivity.

Introduction

The current WHO classification of acute leukemia (AL) has been guided by cytogenetic-molecular entities and their clinical impact. Recurrent molecular-cytogenetic rearrangements serve as both diagnostic markers and as independent prognostic factors for risk group assignment and treatment choice. However, heterogeneous subgroups of leukemia are lacking genetic characterisation, with no clear evidence of differentiation into a single lineage. In addition, some have variable combinations of myeloid and T- or B-cell components (mixed phenotypes). These leukemias, defined by the WHO classification as acute leukemias of ambiguous lineage (ALAL), include acute undifferentiated leukemia, acute leukemias with ambiguous lineage, and mixed phenotype acute leukemias (MPAL).[1] So far, only two cytogenetic markers, i.e. t(9;22)(q34;q22)/*BCR-ABL1* and *KMT2A*-rearrangements, mainly associated with B/myeloid MPAL, have been incorporated to improve diagnosis and risk stratification.[1] Notably, two recent studies have begun to elucidate the genetic basis of pediatric ALAL, and adult MPAL, identifying recurrent genetic and/or epigenetic events overlapping with those found in acute myeloid leukemia (AML), B- or T- acute lymphoblastic leukemia (ALL).[2,3]

An additional WHO entity, termed early T-cell precursor ALL (ETP-ALL), is a subgroup of high-risk T-ALL[4,5] with very immature T progenitor, that retains myeloid differentiation potential.[6] ETP-ALL cases lack a unifying cytogenetic marker.[7]

In this study we focused on 14q32 rearrangements involving *BCL11B*, a transcription factor interacting with the Nucleosome Remodelling and Deacetylase (NuRD) complex,[8,9] which is essential for T-cell development and for maintenance of T-cell identity.[10,11] We found that 14q32 rearrangements activating *BCL11B* are the hallmark of a leukemia entity, named here as "*BCL11B*-a (activated) AL", characterized by expression of both myeloid and T lymphoid antigens with a distinct transcriptomic profile.

Methods

Patients

Patients were recruited from the Hematology Departments, at the University of Perugia, Parma, Bologna, Venezia-Mestre and Avellino Hospitals, Italy; the Centre for Human Genetics, University of Leuven, Belgium; the Leukemia Research Cytogenetics Group, Translational and Clinical Research Institute Newcastle University Centre for Cancer,

Newcastle, UK. All patients or their parents/guardians have provided informed consent for sample collection and its use in approved research studies. This study was approved by the local bio-ethical committee (Bioethics Committees: University of Perugia, number 2014-0259, University of Leuven, number S53745, University Centre for Cancer, Newcastle, number 2007-004013-34, Bioethics Committee of the Kanton of Zurich, number 2014-0383). Molecular analyses were performed in agreement with the Declaration of Helsinki.

Cytogenetics, Fluorescence In Situ Hybridization (FISH), Reverse Transcription Polymerase Chain Reaction (RT-PCR), and Single Nucleotide Polymorphism array (SNPa)

Conventional cytogenetic analysis was performed after G banding (supplemental Material). FISH testing was carried out to refine the 14q32 breakpoints, and breakpoints of chromosome partners, using DNA clones listed in supplemental Table 1 (supplemental Material). RT-PCR and Western blot were performed using standard procedures (supplemental Material). SNPa determined copy number variants (CNV) and copy neutral LOH (cnLOH) (supplemental Material).

Quantitative RT-PCR

Quantitative RT-PCR was used to assess the expression of *BCL11B, SPI1*/PU.1 and *ZEB2*. Details are provided in supplemental Material.

RNA sequencing

RNA-Seq experiments are described in supplemental Material. AML[12] and T-ALL[13] series, that were used as references, belong to the cBioPortal datasets[14,15] (projects TCGA, NEJM 2013 for AML and TARGET, 2018 for T-ALL) and GDC Data Portal datasets[16] (projects TCGA-LAML for AML and TARGET-ALL-P2 for T-ALL). Normalized counts from all *BCL11B*-a AL samples were used for differential expression and Gene Set Enrichment analyses. See supplemental Material for details.

Targeted sequencing and Whole Exome Sequencing (WES)

Gene variants were investigated by targeted sequencing with the Myeloid Solution SOPHiA GENETICS (Saint-Sulpice, Switzerland), that covers 30 relevant genes associated with myeloid hemopathies, and/or by WES (supplemental Material). Sanger sequencing was used to validate next generation sequencing (NGS) findings, and to

study hot-spot mutations, in selected cases. Detailed procedures and the analysis of data are provided in supplemental Material.

Drug sensitivity and resistance profiling

We tested 65 clinical and pre-clinical compounds on five *BCL11B*-a AL samples with available material (case no. 4 with t(2;14); cases nos. 9, 10, and 12 with t(6;14); case no. 18 with t(7;14), Table 1) and compared drug sensitivity with 23 T-ALL.[17] Primary cells were recovered from cryopreserved bone marrow aspirates. Drug responses were assessed in leukemia cells co-cultured on hTERT immortalized primary human bone marrow MSC as previously described.[17] Detailed procedures are provided in supplemental Material.

Data Sharing Statement. All generated data were deposited in NCBI Gene Expression Omnibus (GEO) under accession number GSE162283 (GSE162000 for SNParray, GSE162280 for RNA-Seq and GSE162282 for Sequencing data).

Additional information is provided as supplemental Material.

Results

Identification and molecular characterization of four recurrent 14q32/*BCL11B* translocations

We collected 915 cases with lymphoid and myeloid malignant hemopathies (supplemental Table 2). They included: 96 Chronic Lymphocytic Leukemia, 76 Multiple Myeloma, 96 Myelodysplastic Syndrome, and 646 acute leukemias: 29 Acute Promyelocytic Leukemia, 83 B-ALL, 202 AML (supplemental Table 3), 333 T-ALL (178 non-ETP-ALL, 58 ETP-ALL, 8 T/M MPAL, and 89 not otherwise specified).

FISH screening for *BCL11B*, which is oriented from telomere to centromere and maps centromeric to the *IGH* locus, detected known *BCL11B* rearrangements in T-ALL, i.e. t(5;14)(q35;q32)/*BCL11B-TLX3* (n=45), t(5;14)(q34;q32)/*BCL11B-NKX2.5* (=1), t(7;14)(p15;q32)/*BCL11B-HOXA* (n=1), and inv(14)(q13q32)/*BCL11B-NKX2-1* (n=1). In addition, we found 20 cases [8/202 AML (4%), M0 or M1 subtype, and 12/333 T-ALL (3,6%), including 7 ETP-ALL, 3 T/M MPAL, and 2 T-ALL not otherwise specified] with more telomeric clusters of breakpoints at 14q32/*BCL11B* (Figure 1A, Table 1 and supplemental Table 4) which were all specifically identified by fosmids WI2-2168J13

and WI2-2934J16 (supplemental Figures 1A, 2A, 3A, 4A). The immunophenotype, available in 18 out of 20 cases, showed an immature phenotype in both AML (8/8) and T-ALL (10/10).

Overall, there were four translocations, i.e. t(7;14)(q21.2;q32) (n=2) (supplemental Figure 1A), t(2;14)(q22.3;q32) (n=7) (supplemental Figure 2A), t(6;14)(q25.3;q32) (n=9) (supplemental Figure 3A), and t(8;14)(q24.2;q32) (n=2) (supplemental Figure 4A).

Molecular characterization of t(7;14)(q21.2;q32).

In the two cases with t(7;14)(q21.2;q32), the 14q32 breakpoints were narrowed in between fosmids WI2-2168J13 and WI2-1945I12, a 85Kb region downstream *BCL11B* (Figure 1A). The 7q21.2 breakpoints fell within *CDK6* (Figure 1B). In both cases the full length of *BCL11B* moved to the der(7), at the 3' end of *CDK6* (supplemental Material).

Molecular characterization of t(2;14)(q22.3;q32).

In the seven cases with t(2;14)(q22.3;q32), the 14q32 breakpoints fell between fosmids WI2-2001J18 and WI2-2194I13 (Figure 1A), while the 2q22.3 breakpoints mapped within the Zinc finger E-box Binding homeobox 2 (*ZEB2*) gene (Figure 1C). By cloning and sequencing we found an *in-frame ZEB2-BCL11B* fusion transcript in all cases. While breakpoints in *ZEB2* were alternatively located in exon 2 or 4 (NM_ 014795.3), the breakpoint in *BCL11B* invariably fell in exon 2 (nucleotide 554, NM_138576.3) (supplemental Figure 2B). Therefore, regulation of *BCL11B* transcription moved under the control of the *ZEB2* promoter. The predicted ZEB2-BCL11B proteins retained all the BCL11B functional domains (supplemental Material, supplemental Figure 2C and 2D).

Molecular characterization of t(6;14)(q25.3;q32).

Rearrangements between 6q25.3 and 14q32 consisted of a balanced t(6;14)(q25.3;q32) (n=8) or an ins(6;14)(q25.3;q32q32) (n=1) (Table 1). The 14q32 breakpoints were slightly variable and localized between fosmids WI2-2001J18 and WI2-2934J16 (Figure 1A). The 6q25 breakpoints were detected by clone RP11-19F10 (7 cases) or clone RP11-446N2 (2 cases) in a ~100Kb no-gene region (Figure 1D). In all cases, rearrangements did not produce fusion transcripts but relocated *ARID1B* and its regulatory sequences in close proximity of *BCL11B* at der(6) (case no.10) or der(14) (cases nos. 8, 9, 11-16) (Figure 1D).[18,19]

Molecular characterization of t(8;14)(q24.2;q32).

In the two cases with t(8;14)(q24.2;q32) the 14q32 breakpoints, upstream *BCL11B*, mapped between fosmids WI2-2194I13 and WI2-2934J16 (Figure 1A), while the 8q24.2

breakpoints, telomeric to *MYC,* were narrowed by clone RP11-26E5, which maps ~50kb centromeric of the BENC enhancer region and encompasses *CCDC26*. This clone was retained on der(8) in case no. 19, while it moved to der(14) in case no. 20 (Figure 1E and supplemental Material).

Karyotype was available in 19/20 cases (Table 1) and 14q32/*BCL11B* translocations were detected in 12 cases. In 9 of them the translocation was the only chromosomal change (Table 1). SNPa results were available in 15/20 cases and confirmed a low burden of co-occurring abnormalities (mean: 1.6; range 0-6) (supplemental Table 5). Additional chromosomal abnormalities (ACA), included trisomy 4 in three cases (nos. 2, 12 and 13, Table 1), a 16q deletion encompassing *CTCF* gene in two cases (nos.6 and 17, Table 1), and a del(5q) in one case (no. 4, Table1). Notably, a 4q trisomy has been reported in immature T-ALL by Takahashi et al,[3] and the interstitial deletion of 5q is a recurrent CNV described in ETP-ALL by our group.[20] Moreover, common cnLOH at 2p25.3-p24.1 and 2p22.3-p13.2 (cases nos. 2 and 19), and at 9p24.3-p21 (cases nos. 9 and 20) were found.

Clinical and Phenotypic Features of *BCL11B*-a AL

BCL11B-a AL cases showed male predominance (M/F: 17/3) and a median age of 50.5 years (range: 4-78) (Table 1). Immunophenotypic characterization was available in 16 cases. They all shared an immature immunophenotype characterized by expression of hematopoietic stem cell markers, i.e. HLA-DR, CD117 and/or CD34. All cases shared positivity for the T-lineage surface marker CD2. Fifteen cases were positive for myeloid antigens CD13 and/or CD33; MPO was positive or weak in 8. Positivity for CD7 and for cCD3 was found in 13 and 8 cases, respectively. More mature T-lineage antigens, such as CD1a, CD5 and CD8, were always absent (Table 1).

Overlapping features emerged in six cases that underwent morphological revision of May-Grunwald Giemsa stained bone marrow smears. Blasts were variable in size, with high nuclear/cytoplasmic ratio and agranular cytoplasm. In a variable percentage (20-90%), kidney-shaped nuclei with invagination/indentation, prominent nucleoli and some hand-mirror cells were observed (supplemental Figure 5).

14q32 rearrangements result in *BCL11B* activation

In *BCL11B*-a AL cases, *BCL11B* was activated showing a significant up-regulation compared to AML ($p<0.0001$) and similar levels of expression compared to T-ALL and ETP-ALL cases (Figure 2A). Activation was found at diagnosis but not at hematological

and cytogenetic remission (Figure 2B). Moreover, in the t(2;14) associated *BCL11B*-a AL, a specific test showed low expression of the wild-type *BCL11B,* indicating that up-regulation involved only the fusion transcript (supplemental Figure 6A and 6B). If over-expression was related to one or both alleles in all the other *BCL11B*-a AL could not be determined.

It is worth noting that, in the thymus, *BCL11B* and *SPI1*/PU.1 show an inverse modulation during T-lineage commitment[11,21]. Namely, *SPI1*/PU.1 expression is declining whereas *BCL11B* gene is switching on and progressively increasing. Thus, we investigated *SPI1*/PU.1 levels in our cohort of patients and found that *SPI1*/PU.1 was significantly higher in *BCL11B*-a AL with respect to ETP-ALL ($p=0.009$) and non-ETP T-ALL ($p<0.0001$), while no differences emerged with AML (Figure 2C). We also investigated the expression of *ZEB2* which was rearranged in cases with the t(2;14) translocation. *BCL11B*-a AL showed a significant over-expression of *ZEB2* when compared to T-ALL ($p<0.0001$) and ETP-ALL ($p=0.009$), but not compared to AML (supplemental Figure 7A). Likewise, the single case of t(2;14)/*ZEB2-BCL11B* described by Goossens et al. belonged to the immature subgroup of T-ALL which showed a significantly higher expression of *ZEB2* compared to more mature T-ALL.[22] Moreover we found similar *ZEB2* expression at both diagnosis and remission (supplemental Figure 7B). This may be explained by *ZEB2* expression in the normal myeloid compartment.[23]

A distinct expression profile marks *BCL11B*-a AL cases

Unsupervised analysis of normalized counts obtained from RNA-seq separated *BCL11B*-a AL from T-ALL, ETP-ALL and AML along the first principal component, showing a total variance of 60% (Figure 3A). Differential expression analysis identified 5144 deregulated genes. Up-regulation (4852 up- and 292 down-regulated genes) characterized the signature (Figure 3B). Functional analysis identified the cytokine-cytokine receptor interaction pathway as the most up-regulated. Pathways related to T-cell differentiation, T cell receptor signaling and primary immunodeficiency were the most downregulated (supplemental Table 6). Gene Set Enrichment Analysis showed that BCL11B targets were significantly deregulated in the signature of *BCL11B*-a AL cases (FDR=0.07, Figure 3C). While the analysis of Differentially Expressed Genes (DEGs) revealed a marked skewness towards the upregulation at the global level, the same analysis, focusing on BCL11B direct transcriptional targets, identified an opposite pattern, with a prevalent down-regulation involving 107 out of 179 (60%) known

BCL11B target genes (Figure 3D). This result suggested that 14q32 translocations cause activation of the BCL11B transcriptional repressor program. Although RNA-seq confirmed the hyper-expression of SPI1/PU.1 in *BCL11B*-a AL cases compared to other leukemias, known target genes of PU.1 were not significantly enriched in *BCL11B*-a AL (data not shown).

Compared to the T-ALL series and to ETP-ALL as a separate group, *BCL11B*-a AL cases showed a significant up-regulation of 6265 and 5787 genes, respectively (supplemental Figure 8A and 8B). Functional analysis showed that the cytokine-cytokine receptor interaction was the most up-regulated pathway versus both T-ALL and ETP-ALL. It included positive regulator of JAK/STAT signaling, such as *IFNL1, IFNL3, IFNA, IL6, IL7, IL19, IL20, IL24, IL27, OSMR, IL13RA1,* and *PRLR* (supplemental Table 6). [24,25] A significant down-regulation of 390 genes *vs* T-ALL and of 324 genes vs ETP-ALL was found (supplemental Figure 8A and 8B). Functional analysis identified hematopoietic cell lineage and T-cell receptor signaling as the most down-regulated pathways (supplemental Table 6), suggesting that the T-lymphoid program is not yet fully activated in this immature entity. These pathways included genes encoding T-cell surface antigens (i.e. *CD1A, CD1B, CD1E, CD3D, CD3E, CD3G, CD5, CD8A, CD28*) and for T-cell signaling molecules (*TCF7, LCK, RASGRP1, JUN, RAG1*).

When compared to AML, *BCL11B*-a AL showed up-regulation of 5118 genes and down-regulation of 680 genes (supplemental Figure 8C). Ribosome biogenesis (including genes encoding ribosomal protein subunits) and protein translation pathways (i.e. *EIF3CL* and *EIF4A1*) emerged as the most upregulated (supplemental Table 6).

The mutational landscape of *BCL11B*-a Acute Leukemia

NGS revealed a burden of variants ranging from 2 to 13 per case (mean of 5.7 events). Overall, 95 variants were found in *BCL11B*-a AL cases (Figure 4), 29 of which are not reported in the main variant databases (i.e. gnomAD, dbSNP, 1000 Genome Project, Clinvar, HGMD, Ensembl, COSMIC). For each variant the degree of pathogenicity is shown in supplemental Table 7 and supplemental Material. All investigated cases had *FLT3* mutations, which comprised internal tandem duplication (ITD) (n=12), nucleotide substitution at the tyrosine-kinase domain (TKD, n=4), or both (n=1). No *NOTCH1 or FBXW7* mutations were detected in *BCL11B*-a AL tested (supplemental Material). However, a *NOTCH2* somatic mutation was found in one ETP-ALL case (no 10, supplemental Table 7). *RUNX1* mutations were present in three cases. A variety of

epigenetic modulator genes, namely *WT1* (n=8), *DNMT3A* (n=6), *TET2* (n=4), *EZH2*, *EP300*, and *ASXL2* (n=2, each), were affected in all cases but one (Figure 4 and supplemental Table 7). All other events involving epigenetic genes were not recurrent. In 3 cases, targeted sequencing on paired diagnosis/remission samples, showed that *DNMT3A* mutations remained present in hematological and cytogenetic remission (supplemental Table 8). Additional sporadic variants in genes involved in cell signaling, RNA processing, cell adhesion, cell cycle, and transcriptional regulation were also found (Figure 4 and supplemental Table 7).

BCL11B-a AL are sensitive to tyrosine kinase and JAK/STAT inhibitors

In order to detect functional vulnerabilities, we performed ex vivo drug response profiling in five cases with *BCL11B*-a AL cultured on human mesenchymal stroma cells. Comparing the specific drug sensitivities to an unrelated cohort of T-ALL cases,[17] in *BCL11B*-a AL cases we found a striking decrease of activity for genotoxic agents used in both AML and/or T-ALL, such as docetaxel, mitoxantrone, idarubicin, etoposide, doxorubicin, cytarabine, gemcitabine and topotecan (Figure 5 and supplemental Figure 9). Corroborating the genomic data, that suggest activated FLT3 and JAK/STAT pathways, we found higher sensitivity to tyrosine kinases (sunitinib, crenolanib) and JAK/STAT inhibitors (NVP-BVB808, Momelotinib, Fedratinib, NVP-BSK805) in *BCL11B*-a AL cases compared to other T-ALL samples (Figure 5 and supplemental Figure 9). Of note, the tyrosine kinase inhibitor midostaurin showed low activity in *BCL11B*-a AL cases, despite the presence of *FLT3* mutations, indicating that drug sensitivities may depend on more complex factors than candidate gene mutations (Figure 5 and supplemental Figure 9).

Discussion

In this study, different types of leukemia, variably classified as immature AML, ETP-ALL, or T/M MPAL according to immunophenotype, converged into one genetic disease characterized by 14q32 translocations activating *BCL11B*.

BCL11B is a C_2H_2 zinc-finger transcription factor also defined as a “guardian of T-cell fate”[26] for its role in the maintenance of T-cell identity.[10,11] In human T-ALL, it undergoes translocations alternatively activating *TLX3, HOXA, NKX2-1* and *NKX2-5* genes.[13,27–30] It may also act as a tumour suppressor undergoing loss-of-function mutations and deletions in 13% and 3% of T-ALL and ETP-ALL, respectively.[31] The

physiological expression of *BCL11B* starts in the transition between the stage DN2a to DN2b of the thymocyte and it is maintained along the entire lineage until reaching mature T cells.[11,32] High levels of *BCL11B* have been previously reported in T-cell leukemia/lymphoma (ATLL), T-ALL, and immature AML.[33–35]

From our FISH screening of malignant hemopathies, *BCL11B* was shown to be involved in known T-ALL translocations and in a subset of acute leukemias characterized by recombination of 14q32 with four alternative chromosomes partners, i.e. 2q22.3, 6q25.3, 7q21.2, and 8q24.2. Interestingly, for the last three regions the full-length *BCL11B* translocated to no-gene regions and was likely activated by elements that were previously involved in oncogenesis, namely *ARID1B* super-enhancer at 6q25.3,[18,19,35] a super-enhancer located inside *CDK6* gene, at 7q21.2,[18,28] and the BENC super-enhancer, at 8q24.2.[36,37] Rearrangements involving 2q22.3 as the chromosome partner, instead, generated a *ZEB2-BCL11B* fusion gene, which was highly expressed in the leukemic cells. As a member of the Zinc-finger enhancer binding (ZEB) family ZEB2 controls cellular motility, stem-cell properties, apoptosis and senescence and it is crucial for epithelial mesenchymal transition (EMT).[38] Interestingly, both ZEB2 and BCL11B act as transcriptional repressors by interacting with the NuRD co-repressor complex.[8,9,39,40] As in the fusion protein, ZEB2 maintains its NuRD interaction motif RRKQxxP at N-terminal and BCL11B maintains its C_2H_2-zinc finger DNA binding domain at the C-terminal,[41] an effect of their chimeric product at the transcriptional level is plausible. Here, we found high expression of both genes not only in the leukemic bone marrow of cases bearing the fusion, but also in the other *BCL11B*-a AL cases. However, our results from individual longitudinal analyses pointed to *BCL11B* deregulation as the major pathogenetic event, as *BCL11B*, but not *ZEB2*, decreased at hematological and cytogenetic remission, as expected for clonal driver changes. Nevertheless, since the function of ZEB2 has been emphasized in both myeloid and ETP-ALL leukemogenesis,[22,23] an hypothetical role for *ZEB2* expression in the leukemic process of *BCL11B*-a AL needs to be further investigated.

To provide a diagnostic test to differentiate *BCL11B* activating rearrangements from other typical T-ALL associated translocations,[42] in which known oncogenes are activated by *BCL11B* downstream enhancer,[13,27–30] we set up a specific FISH assay that was shown to be useful to diagnose the new *BCL11B*-a AL entity by discriminating the cluster of breakpoints at the *BCL11B*/14q32 that fall telomeric to the clusters of the other 14q32/*BCL11B* translocations activating oncogenes.

The transcriptome profile grouped the variety of AL with *BCL11B* activation and identified a new entity in which the BCL11B driver effect was emphasized by the impact of its targets within the specific signature. A common phenotypic denominator of these leukemic blasts emerged, with expression of immature, myeloid, and T lymphoid antigens, suggesting potential towards both lymphoid and myeloid programs in the leukemic progenitor. Interestingly, *SPI1*/PU.1 expression in the *BCL11B*-a AL signature was similar to that observed in AML, but significantly higher than the level found in T-ALL. As *SPI1*/PU.1 is a well characterized and double-faced T and myeloid differentiation player, depending on cell context and epigenetics,[43,44] it is a good candidate to support myeloid potential in *BCL11B*-a AL. A putative oncogenic role of *SPI1*/PU.1 in this leukemia subset, is suggested by the occurrence of recurrent *SPI1*/PU.1 fusions in immature T-ALL. [43,45]

Focusing on the mutational landscape, both *FLT3* and epigenetic genes were affected in the *BCL11B*-a AL cases. Interestingly, *WT1, DNMT3A* and *TET2*, the most frequently mutated epigenetic genes in this study, have been previously reported in acute leukemia with expression of myeloid and/or T-lymphoid antigens.[46–48] Furthermore, persistence of *DNMT3A* gene mutations at remission has been described in both AML[49] and T-ALL.[50] These findings suggest that *DNMT3A* mutations identify preleukemic clonal hematopoiesis underlying development of different leukemia subtypes.[48] With respect to *FLT3* mutations, including the ITD and D835 variants, they did not discriminate immunological and cytogenetic leukemia subsets. However, they have been traced as important second hits, so-called class II mutations, supporting malignant proliferation.[48,51] Remarkably, *in vivo* mouse models showed that, when combined, *FLT3-ITD* and *DNMT3A* loss-of-function mutations recapitulated a variety of human leukemias, including mixed-lineage leukemia expressing both myeloid and T cell markers.[52] Altogether these findings suggest a three hits model in the pathogenesis of *BCL11B*-a AL, in which epigenetic event(s) may act by opening the chromatin in a totipotent progenitor, thus favoring *BCL11B* rearrangements, and *FLT3* mutations behave as a crucial hit to support proliferation.[48]

Functional drug response further supported the specific biologic profile of *BCL11B*-a AL, and provided some new insights. In addition to a poor sensitivity to genotoxic agents used in either AML and T-ALL induction therapy, a higher sensitivity to distinct tyrosine kinase and JAK/STAT pathway inhibitors emerged. While lack of sensitivity to genotoxic

agents appears unpredicted by genomic lesions, they are instead in keeping with sensitivity to JAK/STAT and tyrosine kinase inhibition.

In conclusion, in this new leukemia entity genomic findings overstep immunological classification of immature blasts, providing new insights for precise diagnosis and hopefully for tailored therapy in prospective clinical trials.

Acknowledgements

C.M. was supported by PRIN2017 code 2017PPS2X4. J.P.B. and B.B. were supported by Empiris Foundation. We are grateful to Doctor Lucia Brandimarte for her invaluable help during the development of this work.

Authorship

Contributions: C.M., R.L.S., V.P., Si.A. and M.M. performed and analyzed cytogenetics, FISH, and SNP arrays. D.D.G., P.G., F.P., Ca.M., Z.K.A., K.D.K., S.A., J.C. and R.P. performed and analyzed molecular and NGS studies. C.M., R.L.S., C.H., N.T., G.D.S., G.R., R.B. and P.V.B. collected samples and patient data. B.B. and J.P.B. performed drug profile. C.M. conceived the study. C.M., D.D.G. and R.L.S. collected all data and wrote the manuscript.

Conflict of interest disclosures

The authors declare no competing financial interest.

References

1. Swerdlow SH, Campo E, Harris NL, et al. WHO Classification of Tumours of Haematopoietic and Lymphoid Tissues. Lyon, France. 2017.
2. Alexander TB, Gu Z, Iacobucci I, et al. The genetic basis and cell of origin of mixed phenotype acute leukaemia. *Nature*. 2018;562(7727):373–379.
3. Takahashi K, Wang F, Morita K, et al. Integrative genomic analysis of adult mixed phenotype acute leukemia delineates lineage associated molecular subtypes. *Nat. Commun.* 2018;9(1):2670.
4. Patrick K, Wade R, Goulden N, et al. Outcome for children and young people with Early T-cell precursor acute lymphoblastic leukaemia treated on a contemporary protocol, UKALL 2003. *Br. J. Haematol.* 2014;166(3):421–424.
5. Conter V, Valsecchi MG, Buldini B, et al. Early T-cell precursor acute lymphoblastic leukaemia in children treated in AIEOP centres with AIEOP-BFM protocols: a retrospective analysis. *Lancet Haematol.* 2016;3(2):e80–e86.
6. Coustan-Smith E, Mullighan CG, Onciu M, et al. Early T-cell precursor leukaemia: a subtype of very high-risk acute lymphoblastic leukaemia. *Lancet Oncol.* 2009;10(2):147–156.
7. Zhang J, Ding L, Holmfeldt L, et al. The genetic basis of early T-cell precursor acute lymphoblastic leukaemia. *Nature*. 2012;481(7380):157–163.
8. Cismasiu VB, Adamo K, Gecewicz J, et al. BCL11B functionally associates with the NuRD complex in T lymphocytes to repress targeted promoter. *Oncogene*. 2005;24(45):6753–6764.
9. Dubuissez M, Loison I, Paget S, et al. Protein Kinase C-Mediated Phosphorylation of BCL11B at Serine 2 Negatively Regulates Its Interaction with NuRD Complexes during CD4 + T-Cell Activation. *Mol. Cell. Biol.* 2016;36(13):1881–1898.
10. Liu P, Li P, Burke S. Critical roles of Bcl11b in T-cell development and maintenance of T-cell identity. *Immunol. Rev.* 2010;238(1):138–149.
11. Rothenberg E V. Programming for T-lymphocyte fates: modularity and mechanisms. *Genes Dev.* 2019;33(17–18):1117–1135.
12. The Cancer Genome Atlas Research Network. Genomic and Epigenomic Landscapes of Adult De Novo Acute Myeloid Leukemia. *N. Engl. J. Med.* 2013;368(22):2059–2074.
13. Liu Y, Easton J, Shao Y, et al. The genomic landscape of pediatric and young

adult T-lineage acute lymphoblastic leukemia. *Nat. Genet.* 2017;49(8):1211–1218.

14. Cerami E, Gao J, Dogrusoz U, et al. The cBio Cancer Genomics Portal: An Open Platform for Exploring Multidimensional Cancer Genomics Data. *Cancer Discov.* 2012;2(5):401–404.
15. Gao J, Aksoy BA, Dogrusoz U, et al. Integrative Analysis of Complex Cancer Genomics and Clinical Profiles Using the cBioPortal. *Sci. Signal.* 2013;6(269):pl1–pl1.
16. Grossman RL, Heath AP, Ferretti V, et al. Toward a Shared Vision for Cancer Genomic Data. *N. Engl. J. Med.* 2016;375(12):1109–1112.
17. Frismantas V, Dobay MP, Rinaldi A, et al. Ex vivo drug response profiling detects recurrent sensitivity patterns in drug-resistant acute lymphoblastic leukemia. *Blood*. 2017;129(11):e26–e37.
18. Hnisz D, Abraham BJ, Lee TI, et al. Super-Enhancers in the Control of Cell Identity and Disease. *Cell*. 2013;155(4):934–947.
19. Wang W, Beird H, Kroll CJ, et al. T(6;14)(q25;q32) involves BCL11B and is highly associated with mixed-phenotype acute leukemia, T/myeloid. *Leukemia*. 2020;34(9):2509–2512.
20. La Starza R, Barba G, Demeyer S, et al. Deletions of the long arm of chromosome 5 define subgroups of T-cell acute lymphoblastic leukemia. *Haematologica*. 2016;101(8):951–958.
21. Rothenberg E V., Hosokawa H, Ungerbäck J. Mechanisms of Action of Hematopoietic Transcription Factor PU.1 in Initiation of T-Cell Development. *Front. Immunol.* 2019;10:.
22. Goossens S, Radaelli E, Blanchet O, et al. ZEB2 drives immature T-cell lymphoblastic leukaemia development via enhanced tumour-initiating potential and IL-7 receptor signalling. *Nat. Commun.* 2015;6(1):5794.
23. Li J, Riedt T, Goossens S, et al. The EMT transcription factor Zeb2 controls adult murine hematopoietic differentiation by regulating cytokine signaling. *Blood*. 2017;129(4):460–472.
24. Baker SJ, Rane SG, Reddy EP. Hematopoietic cytokine receptor signaling. *Oncogene*. 2007;26(47):6724–6737.
25. Hammarén HM, Virtanen AT, Raivola J, Silvennoinen O. The regulation of JAKs in cytokine signaling and its breakdown in disease. *Cytokine*. 2019;118:48–63.

26. Di Santo JP. A Guardian of T Cell Fate. *Science.* 2010;329(5987):44–45.
27. Nagel S, Kaufmann M, Drexler HG, MacLeod RAF. The cardiac homeobox gene NKX2-5 is deregulated by juxtaposition with BCL11B in pediatric T-ALL cell lines via a novel t(5;14)(q35.1;q32.2). *Cancer Res.* 2003;63(17):5329–5334.
28. Su XY, Busson M, Della Valle V, et al. Various types of rearrangements targetTLX3 locus in T-cell acute lymphoblastic leukemia. *Genes, Chromosom. Cancer*. 2004;41(3):243–249.
29. Su X, Drabkin H, Clappier E, et al. Transforming potential of the T-cell acute lymphoblastic leukemia-associated homeobox genesHOXA13,TLX1, andTLX3. *Genes, Chromosom. Cancer*. 2006;45(9):846–855.
30. Nagel S, Scherr M, Kel A, et al. Activation of TLX3 and NKX2-5 in t(5;14)(q35;q32) T-Cell Acute Lymphoblastic Leukemia by Remote 3'-BCL11B Enhancers and Coregulation by PU.1 and HMGA1. *Cancer Res.* 2007;67(4):1461–1471.
31. De Keersmaecker K, Real PJ, Gatta G Della, et al. The TLX1 oncogene drives aneuploidy in T cell transformation. *Nat. Med.* 2010;16(11):1321–1327.
32. Kadoch C, Hargreaves DC, Hodges C, et al. Proteomic and bioinformatic analysis of mammalian SWI/SNF complexes identifies extensive roles in human malignancy. *Nat. Genet.* 2013;45(6):592–601.
33. Oshiro A. Identification of subtype-specific genomic alterations in aggressive adult T-cell leukemia/lymphoma. *Blood*. 2006;107(11):4500–4507.
34. Przybylski GK, Dik WA, Wanzeck J, et al. Disruption of the BCL11B gene through inv(14)(q11.2q32.31) results in the expression of BCL11B-TRDC fusion transcripts and is associated with the absence of wild-type BCL11B transcripts in T-ALL. *Leukemia*. 2005;19(2):201–208.
35. Abbas S, Sanders MA, Zeilemaker A, et al. Integrated genome-wide genotyping and gene expression profiling reveals BCL11B as a putative oncogene in acute myeloid leukemia with 14q32 aberrations. *Haematologica*. 2014;99(5):848–857.
36. Lovén J, Hoke HA, Lin CY, et al. Selective Inhibition of Tumor Oncogenes by Disruption of Super-Enhancers. *Cell*. 2013;153(2):320–334.
37. Bahr C, von Paleske L, Uslu V V., et al. A Myc enhancer cluster regulates normal and leukaemic haematopoietic stem cell hierarchies. *Nature*. 2018;553(7689):515–520.
38. Lamouille S, Xu J, Derynck R. Molecular mechanisms of epithelial–mesenchymal

transition. *Nat. Rev. Mol. Cell Biol.* 2014;15(3):178–196.

39. Verstappen G, van Grunsven LA, Michiels C, et al. Atypical Mowat-Wilson patient confirms the importance of the novel association between ZFHX1B/SIP1 and NuRD corepressor complex. *Hum. Mol. Genet.* 2008;17(8):1175–1183.
40. Si W, Huang W, Zheng Y, et al. Dysfunction of the Reciprocal Feedback Loop between GATA3- and ZEB2-Nucleated Repression Programs Contributes to Breast Cancer Metastasis. *Cancer Cell*. 2015;27(6):822–836.
41. Avram D, Fields A, Top KPO, et al. Isolation of a Novel Family of C 2 H 2 Zinc Finger Proteins Implicated in Transcriptional Repression Mediated by Chicken Ovalbumin Upstream Promoter Transcription Factor (COUP-TF) Orphan Nuclear Receptors. *J. Biol. Chem.* 2000;275(14):10315–10322.
42. La Starza R, Pierini V, Pierini T, et al. Design of a Comprehensive Fluorescence in Situ Hybridization Assay for Genetic Classification of T-Cell Acute Lymphoblastic Leukemia. *J. Mol. Diagnostics*. 2020;22(5):629–639.
43. Homminga I, Pieters R, Langerak AW, et al. Integrated Transcript and Genome Analyses Reveal NKX2-1 and MEF2C as Potential Oncogenes in T Cell Acute Lymphoblastic Leukemia. *Cancer Cell*. 2011;19(4):484–497.
44. Pundhir S, Bratt Lauridsen FK, Schuster MB, et al. Enhancer and Transcription Factor Dynamics during Myeloid Differentiation Reveal an Early Differentiation Block in Cebpa null Progenitors. *Cell Rep.* 2018;23(9):2744–2757.
45. Seki M, Kimura S, Isobe T, et al. Recurrent SPI1 (PU.1) fusions in high-risk pediatric T cell acute lymphoblastic leukemia. *Nat. Genet.* 2017;49(8):1274–1281.
46. Peirs S, Van der Meulen J, Van de Walle I, et al. Epigenetics in T-cell acute lymphoblastic leukemia. *Immunol. Rev.* 2015;263(1):50–67.
47. Pronier E, Bowman RL, Ahn J, et al. Genetic and epigenetic evolution as a contributor to WT1-mutant leukemogenesis. *Blood*. 2018;132(12):1265–1278.
48. Shlush LI, Zandi S, Mitchell A, et al. Identification of pre-leukaemic haematopoietic stem cells in acute leukaemia. *Nature*. 2014;506(7488):328–333.
49. Gaidzik VI, Weber D, Paschka P, et al. DNMT3A mutant transcript levels persist in remission and do not predict outcome in patients with acute myeloid leukemia. *Leukemia*. 2018;32(1):30–37.
50. Bond J, Touzart A, Leprêtre S, et al. DNMT3A mutation is associated with increased age and adverse outcome in adult T-cell acute lymphoblastic leukemia. *Haematologica*. 2019;104(8):1617–1625.

51. Gilliland DG, Griffin JD. The roles of FLT3 in hematopoiesis and leukemia. *Blood*. 2002;100(5):1532–1542.
52. Yang L, Rodriguez B, Mayle A, et al. DNMT3A Loss Drives Enhancer Hypomethylation in FLT3-ITD-Associated Leukemias. *Cancer Cell*. 2016;29(6):922–934.

Tables

Table 1. Details of *BCL11B*-a AL cases

No.	Code	*Sex/Age (y)*	*FAB/WHO diagnosis*	*Immunophenotype*	*Karyotype*
t(2;14)(q22;q32)					
1	UPN#455	M/72	AML	n.a.	46,XY,**t(2;14)(q22;q32)**[4]/46,XY[9]
2	UPN#456	M/52	T/myeloid MPAL	**CD2+, CD117+**, **CD34+**, **HLA-DR+, CD13+**, TdT+, cCD3+, CD56+, MPO+, cCD79a+, CD7-, CD3-, CD5-, CD33-, CD14-, CD15-, CD22-, CD20-	46,XY,**t(2;14)(q22;q32)**[19]/47,idem,+4[3]
3	UPN#457	M/37	AML M0	**CD2+, CD117+**, **CD34+**, **HLA-DR+, CD13+**, TdT+, CD7+, CD15+, MPO+/-, CD33+/-, CD14-, CD11c-, CD3-, CD4-, CD8-, CD5-, CD10-, CD19-	46,XY,**t(2;14)(q22;q32)**[15]
4	UPN#141	F/76	AML M0	**CD2+, CD117+**, **CD34+**, **HLA-DR+, CD13+**, CD7+, MPO+, CD11b+, CD38+, CD33-, CD14-, CD15-, cCD3-, CD3-, CD4-, CD56-, CD10-, cCD79a-, CD19-	46,XX,**t(2;14)(q22;q32)**,del(5)(q13q31)[15]
5	UPN#458	F/68	AML M1	**CD2+, CD117+**, **CD34+**, **HLA-DR+, CD13+**, CD7+, MPO+/-, CD33+, CD14-, TdT-, CD3-, CD4-, CD8-, CD1a-, CD10-, CD19-, CD22-	46,XX,**t(2;14)(q22;q32)**[12]/46,idem,add(12)(q24)[5]/46,XX[3]
6	UPN#151	M/18	AML M1	**CD2+, CD117+, CD34+, HLA-DR+, CD13+**, CD15+, CD56+, MPO-, CD33-, CD14-, CD7-, cCD3-, CD3-, CD4-, CD5-, CD19-, cCD79a-	46,XY,**t(2;14)(q22;q32)**,del(16)(q21)[15]
7	UPN#459	M/64	ETP-ALL	**CD2+, CD117+, CD34+, HLA-DR+, CD13+,** CD11b+, CD56+, TdT+, CD7+, CD38+, cCD3+, MPO-, CD33-, CD4-, CD5-, CD1a-, CD10-, CD19-, CD20-, cCD79a-	46,XY[24]**.ish t(2;14)(q22;q32)(WI2-2194I13+;WI2-2001J18+)**[5]
t(6;14)(q25;q32)					
8	UPN#143	M/17	AML-M1	**CD2+, CD117+**, **CD34+**, **HLA-DR+, CD13+**, TdT+, CD33+, MPO+, CD56+, CD15+, CD14-, CD7-, cCD3-, CD3-, CD4-, CD5-, CD10-, CD19-, CD20-, cCD79a-	46,XY,**t(6;14)(q25;q32)**[15]
9	UPN#145	M/59	T/myeloid MPAL	**CD2+, CD117+**, **CD34+**, **CD13+**, CD7+, TdT+, cCD3+, CD3-, CD8-, CD4-, CD5-, CD1a-, CD10-, cCD79a- **CD2+, CD13+, CD33+**, CD11b+, MPO+, CD14+, CD34-, CD117-, CD10-, cCD79a-	46,XY,**t(6;14)(q25;q32)**,del(11)(p13p15)[15]
10	UPN#460	M/48	ETP-ALL	**CD2+, CD117+**, **CD34+**, **HLA-DR+, CD13+**, CD7+, TdT+, CD33+, CD38+, CD45+, CD99+, CD133+, cCD3+, CD3-, CD4-, CD5-, CD8-, CD52-, CD56-, CD65-, CD79a-, MPO-, TCR A/B-, TCR G/D-, CD10-, CD19-, cCD79a-	46,XY,add(19)(q13)[10]/46,XY[5]**.ish ins(6;14)(q25;q32q32)(WI2-2194I13+;WI2-2934J16+)**[6]
11	UPN#260	M/4	ETP-ALL	**CD2+, CD117+, CD34+, HLA-DR+, CD33+,** CD7+, TdT+, CD38+, CD45+, cCD3+, CD11b+, MPO+/-, CD99+ CD3-, CD4-, CD5-, CD8-, CD1a-, CD56-, CD13-, CD14-, CD14-, CD65-, CD10-, CD19-	46,XY[10]**.ish t(6;14)(q25;q32)(WI2-2194I13+;WI2-2001J18+)**[5]
12	UPN#462	F/78	ETP-ALL	**CD2+, CD117+, CD34+, HLA-DR+, CD13+,** CD7+, CD38+, cCD3+, TdT-, CD4-, CD8-, CD3-, CD5-, CD56-, CD79a-, CD15-, CD33-, MPO-, CD61-, CD10-, CD19-, CD20-, CD22-, cCD79a-	47,XX,+4[8]/46,XX[8].**nuc ish(WI2-2001J18X2),(WI2-2194I13X2),(WI2-2001J18 sep WI2-2194I13X1)**[70/100]

13	UPN#463	M/18	T-ALL unspecified	n.a.	47,XY,+4[15]/46,XY[15]**.ish t(6;14)(q25;q32)(WI2-2194I13+;WI2-2001J18+)**[3]
14	UPN#464	M/29	T-ALL unspecified	n.a.	**nuc ish(WI2-2001J18X2),(WI2-2194I13X2),(WI2-2001J18 sep WI2-2194I13X1)**[70/106]
15	UPN#465	M/12	ETP-ALL	n.a.	46,XY**,t(6;14)(q25;q32),**del(12)(p11p13)[9]/46,XY[6]
16	UPN#466	M/44	ETP-ALL	**CD2+, CD117+, CD34+, HLA-DR+, CD13+,** CD7+, CD38+, TdT+, CD33-, sCD3-, CD4-, CD8-, CD5-, CD56-, CD10-, CD19-	46,XY**,t(6;14)(q25;q32)**[9]/46,XY[3]
t(7;14)(q22;q32)					
17	UPN#149	M/51	ETP-ALL	**CD2+, CD117+, CD34+**, **HLA-DR+/-,** cCD3+, TdT+, CD7+/-, CD15+/-, sCD3-, CD5-, CD4-, CD8-, MPO-, CD13-, CD33-, CD10-, cCD79a-	46,XY,**t(7;14)(q21;q32)**[16]/46,XY[5]
18	UPN#147	M/50	T/myeloid MPAL	**CD2+, CD117+, CD34+, HLA-DR+**, CD7+, CD38+, CD15+ **CD3+, CD2+, CD117+, CD34+, HLA-DR+**, **CD33dim, CD13dim**, CD7+, CD38+, CD15+, MPO+, CD36+, CD123+, CD10-, CD19-, CD22-, cCD79a-	46,XY,**t(7;14)(q21;q32)**[9]/46,XY[1]
t(8;14)(q24;q32)					
19	UPN#461	M/65	AML M0	**CD2+, CD117+, CD34+, HLA-DR+/-, CD13+**, CD7+, cCD3-, CD3-, CD4-, CD1a-, CD5-, CD8-, MPO-, TdT-, CD10-, CD19-	46,XY,t(2;5)(p21;q13)[10]/46,XX[9].**nuc ish(WI2-2194I13X2),(WI2-2934J16X2),(WI2-2194I13 sep WI2-2934J16)[100/120]**
20	UPN#467	M/51	AML M0	**CD2+, CD117+, CD34+, HLA-DR+, CD13+**, CD7+, MPO-, CD33-, cCD3-, CD3-, CD8-, CD5-, CD56-, CD19-, cCD79a-	46,XY[10].**nuc ish(WI2-2194I13X2),(WI2-2934J16X2),(WI2-2194I13 sep WI2-2934J16)**[91/100]

n.a. not available

Figure Legends

Figure 1. Breakpoints characterization in *BCL11B*-a AL. (A) Break-apart FISH assay differentiating t(2;14), t(6;14), t(7;14), and t(8;14) translocations (fosmid WI2-2168J13, red and fosmid WI2-293J16, green) from four known rearrangements in T-ALL. The thin black horizontal lines represent fosmids that were used to narrow the 14q32 breakpoints. Arrows indicate the mapping of breakpoint in each case. Mapping of breakpoints at: (B) *CDK6*/7q21.2; (C) *ZEB2*/2q22.3; (D) 6q25.3; and (E) 8q24. Patient numbers refer to Table 1. Figures not to scale. SE, super-enhancer.

Figure 2. 14q32 rearrangements result in the activation of *BCL11B* and *SPI1*/PU.1. (A) Expression of *BCL11B* in 15 *BCL11B*-a AL cases (nos. 1-4, 6-13, 17-18, 20, Table 1) compared to in-house AML (n=19), ETP-ALL (n=8) and T-ALL (n=15) series. (B) One of three independent experiments showing longitudinal expression of *BCL11B* in six paired diagnosis-remission *BCL11B*-a AL cases: case no 4 (black), case no 6 (blue), case no 8 (red), case no 9 (green), case no 17 (light blue), case no 18 (violet). Patient numbers refer to Table 1. (C) Expression of *SPI1*/PU.1 in 15 *BCL11B*-a cases (nos. 1-4, 6-13, 17-18, 20, Table 1) compared to in-house AML (n=19), ETP-ALL (n=7) and T-ALL (n=15) series. ns, not significant. Values are expressed as means ± SEM. Cp, crossing point.

Figure 3. Distinct expression profile in *BCL11B*-a AL. (A) Scatter plot showing variance distribution of *BCL11B*-a AL, AML, ETP-ALL, and T-ALL cases emphasized by principal component analysis 1 (PC1). (B) Volcano plot showing the gene expression in *BCL11B*-a AL casess compared to AML, ETP-ALL, and T-ALL. Log_2FC is plotted against the $-Log_{10}$ padj. Black indicates genes with significant FDR (≤0.05). Red and blue represent up-and down-regulated DEGs, respectively (FDR≤0.05, |Log2FC|≥2). Gray, not significant genes. (C) Gene Set Enrichment Analysis of BCL11B target genes in *BCL11B*-a AL cases *versus* other leukemic groups (AML, ETP-ALL and T-ALL). (D) Volcano plot showing the distribution of 350 BCL11B targets in *BCL11B*-a AL cases compared to other leukemias. Log_2FC is plotted against the $-Log_{10}$padj. Red and blue represent significant (FDR ≤0.05) up- and down-regulated targets, respectively. FDR, False Discovery Rate; NES, Normalized Enrichment Score; FC, Fold Change.

Figure 4. Mutational profile of *BCL11B*-a AL. Oncoprint heatmap showing all sequence variants detected in *BCL11B*-a AL cases. In addition to somatic mutations

(dark green), variants in which the somatic or germline origin could not be definitively assessed (light green) are indicated. Additional gene alterations are shown by different colors. Mutational analysis was not performed in cases nos. 15 and 19 due to lack of material. cnLOH, copy number Loss of Heterozygosity.

Figure 5. Drug response profile of *BCL11B*-a AL. Heatmap indicating the response of *BCL11B-a* AL (5 cases, nos. 4, 9, 10, 12, 18) compared to T-ALL (23 cases)[17] to 65 compounds and represented by IC_{50} values. Samples (rows) were ordered according to clinical classification (*BCL11B*-a AL and T-ALL), and compounds were reported in columns.

Figure 1

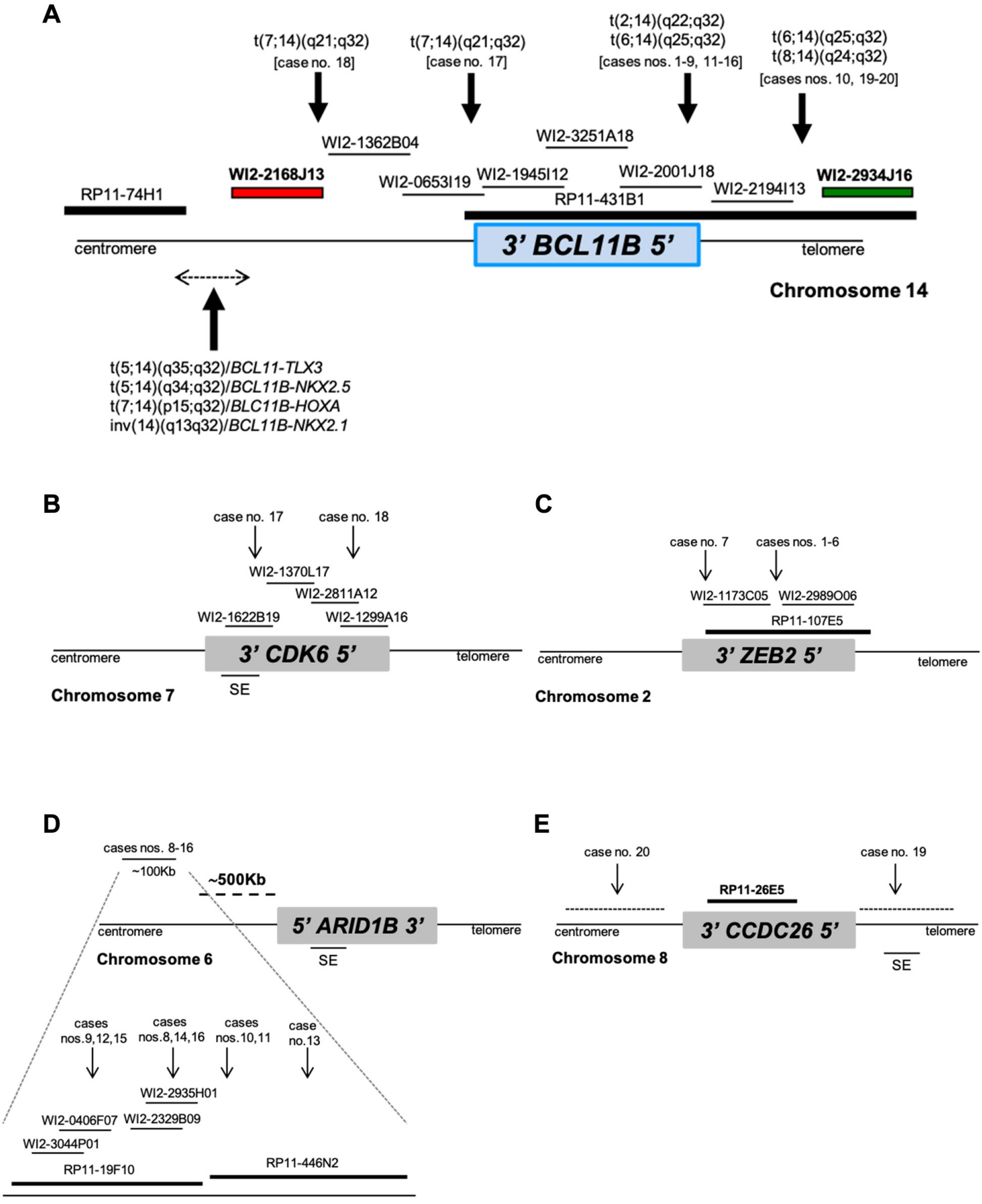
A
t(7;14)(q21;q32)
[case no. 18]
t(7;14)(q21;q32)
[case no. 17]
t(2;14)(q22;q32)
t(6;14)(q25;q32)
[cases nos. 1-9, 11-16]
t(6;14)(q25;q32)
t(8;14)(q24;q32)
[cases nos. 10, 19-20]
WI2-1362B04
WI2-3251A18
WI2-2168J13
WI2-0653I19
WI2-1945I12
WI2-2001J18
WI2-2194I13
WI2-2934J16
RP11-74H1
RP11-431B1
centromere
3' BCL11B 5'
telomere
Chromosome 14
t(5;14)(q35;q32)/BCL11-TLX3
t(5;14)(q34;q32)/BCL11B-NKX2.5
t(7;14)(p15;q32)/BLC11B-HOXA
inv(14)(q13q32)/BCL11B-NKX2.1
B
case no. 17
case no. 18
WI2-1370L17
WI2-2811A12
WI2-1622B19
WI2-1299A16
centromere
3' CDK6 5'
telomere
SE
Chromosome 7
C
case no. 7
cases nos. 1-6
WI2-1173C05
WI2-2989O06
RP11-107E5
centromere
3' ZEB2 5'
telomere
Chromosome 2
D
cases nos. 8-16
~100Kb
~500Kb
centromere
5' ARID1B 3'
telomere
SE
Chromosome 6
cases nos.9,12,15
cases nos.8,14,16
cases nos.10,11
case no.13
WI2-2935H01
WI2-0406F07
WI2-2329B09
WI2-3044P01
RP11-19F10
RP11-446N2
E
case no. 20
case no. 19
RP11-26E5
centromere
3' CCDC26 5'
telomere
SE
Chromosome 8

Figure 2

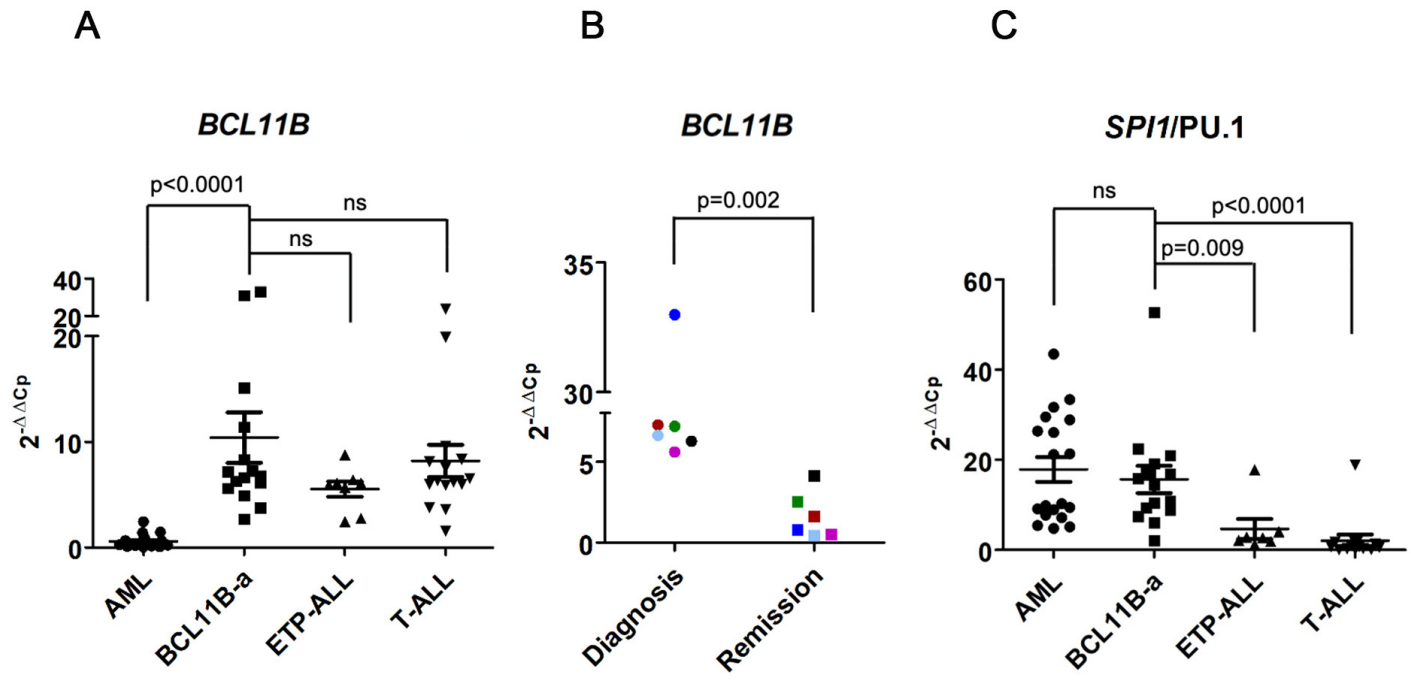
A
BCL11B
p<0.0001
ns
ns
40
20
20
10
0
2-ΔΔCp
AML
BCL11B-a
ETP-ALL
T-ALL
B
BCL11B
p=0.002
35
30
5
0
2-ΔΔCp
Diagnosis
Remission
C
SPI1/PU.1
ns
p<0.0001
p=0.009
60
40
20
0
2-ΔΔCp
AML
BCL11B-a
ETP-ALL
T-ALL

Figure 3

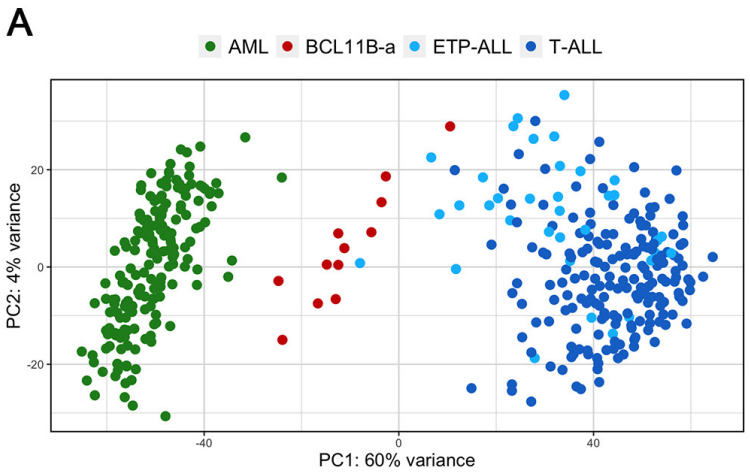
A
AML
BCL11B-a
ETP-ALL
T-ALL
PC2: 4% variance
PC1: 60% variance

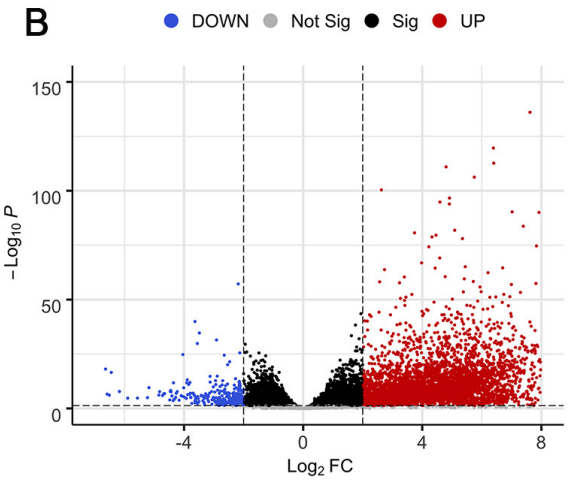
B
DOWN
Not Sig
Sig
UP
−Log10 P
Log2 FC

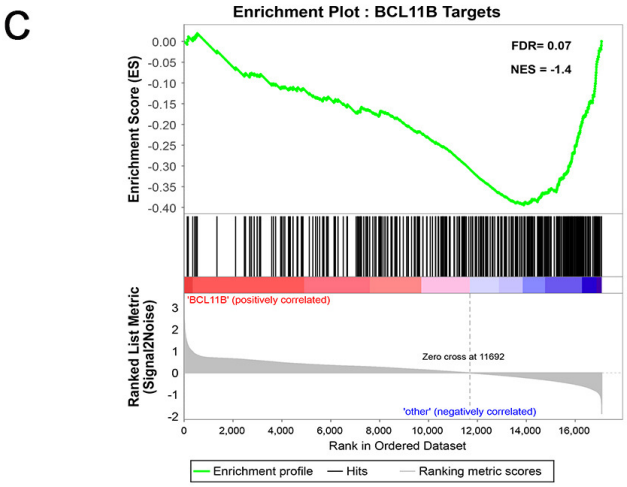
C
Enrichment Plot : BCL11B Targets
FDR= 0.07
NES = -1.4
Enrichment Score (ES)
'BCL11B' (positively correlated)
Ranked List Metric (Signal2Noise)
Zero cross at 11692
'other' (negatively correlated)
Rank in Ordered Dataset
Enrichment profile
Hits
Ranking metric scores

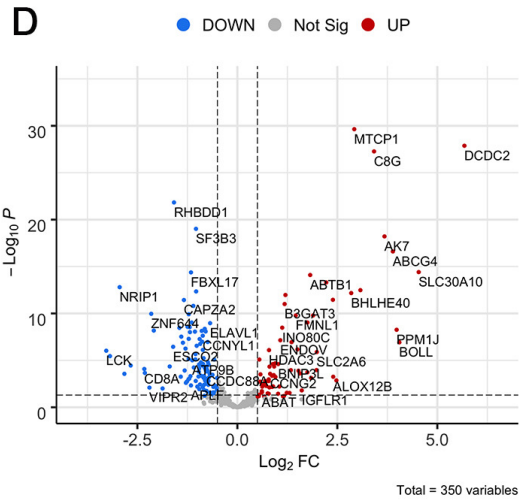
D
DOWN
Not Sig
UP
−Log10 P
Log2 FC
Total = 350 variables

Figure 4


Signaling
Epigenetic
RNA processing
Cell Adhesion
Cell Cycle
Transcription
Other
FLT3
GNAS
PTPN11
PTPN13
EGFR
NOTCH2
SAV1
STAT5A
KALRN
KHDRBS2
CXCR4
Signaling
WT1
DNMT3A
TET2
EZH2
EP300
ASXL2
KMT2C
KMT2D
SETD2
NCOR1
Epigenetic
SRSF2
U2AF1
RNA processing
FAT4
FAT2
EZR
BOC
CDH1
CDH10
Cell Adhesion
CDKN2A
RB1
NUMA1
LATS1
Cell Cycle
RUNX1
HOXA1
MSI2
ZNF557
PRRX1
Transcription
TNFAIP3
TTN
ZMYM3
ATXN7L1
MDN1
KIAA1958
MAGEF1
PLAA
MYH11
MSH2
Other
Case.1
Case.2
Case.3
Case.4
Case.5
Case.6
Case.7
Case.8
Case.9
Case.10
Case.11
Case.12
Case.13
Case.14
Case.16
Case.17
Case.18
Case.20
t(2;14)
t(6;14)
t(7;14)
t(8;14)
Gene Alterations
somatic mutation
variant of unknown status
loss
cnLOH
not available
single alteration
multiple alterations

Figure 5

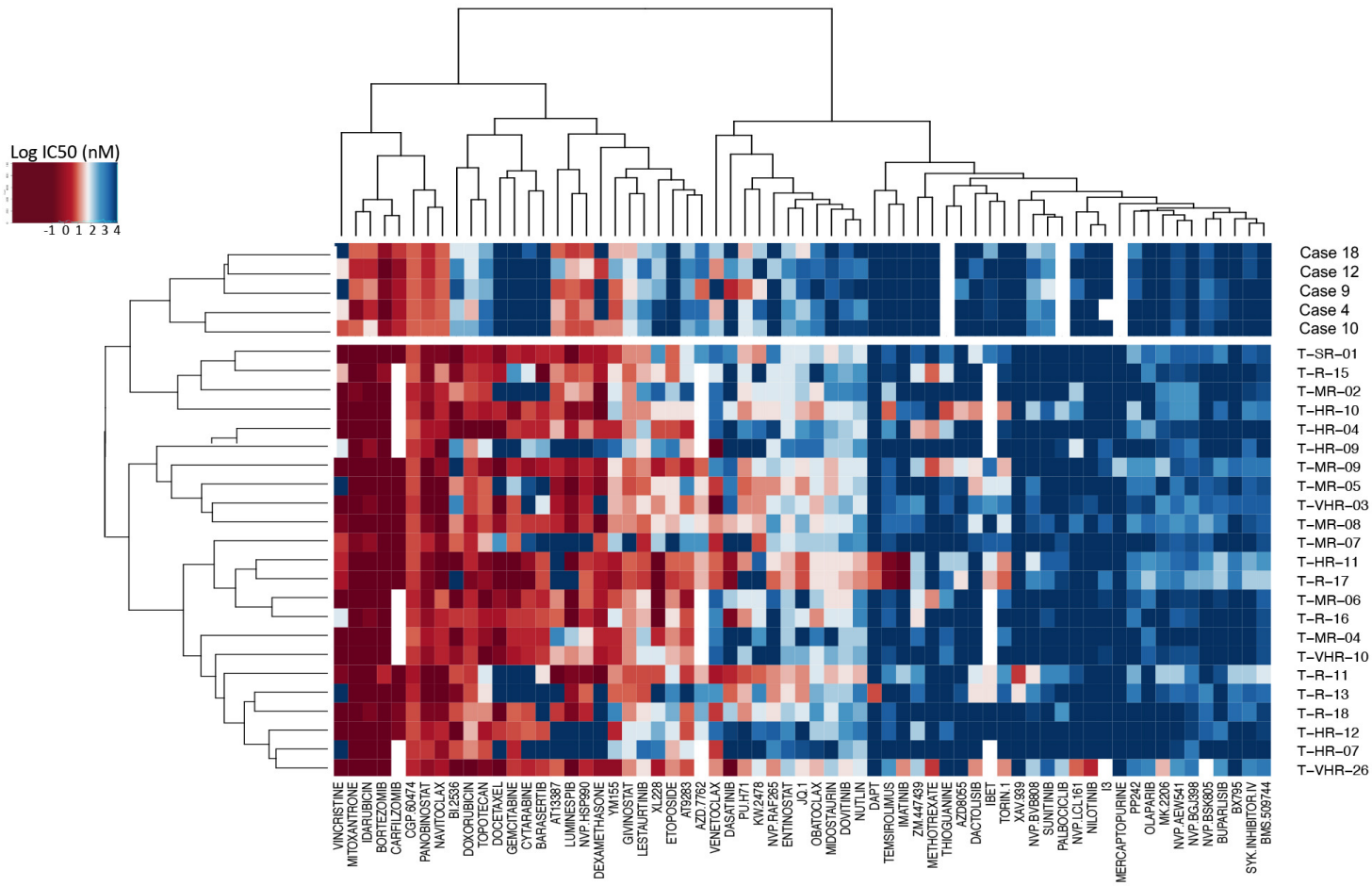
Log IC50 (nM)
-1 0 1 2 3 4
Case 18
Case 12
Case 9
Case 4
Case 10
T−SR−01
T−R−15
T−MR−02
T−HR−10
T−HR−04
T−HR−09
T−MR−09
T−MR−05
T−VHR−03
T−MR−08
T−MR−07
T−HR−11
T−R−17
T−MR−06
T−R−16
T−MR−04
T−VHR−10
T−R−11
T−R−13
T−R−18
T−HR−12
T−HR−07
T−VHR−26
VINCRISTINE
MITOXANTRONE
IDARUBICIN
BORTEZOMIB
CARFILZOMIB
CGP.60474
PANOBINOSTAT
NAVITOCLAX
BI.2536
DOXORUBICIN
TOPOTECAN
DOCETAXEL
GEMCITABINE
CYTARABINE
BARASERTIB
AT13387
LUMINESPIB
NVP.HSP990
DEXAMETHASONE
YM155
GIVINOSTAT
LESTAURTINIB
XL228
ETOPOSIDE
AT9283
AZD.7762
VENETOCLAX
DASATINIB
PLX.H71
KW.2478
NVP.RAF265
ENTINOSTAT
JQ.1
OBATOCLAX
MIDOSTAURIN
DOVITINIB
NUTLIN
DAPT
TEMSIROLIMUS
IMATINIB
ZM.447439
METHOTREXATE
THIOGUANINE
AZD8055
DACTOLISIB
IBET
TORIN.1
XAV.939
NVP.BVB808
SUNITINIB
PALBOCICLIB
NVP.LCL161
NILOTINIB
I3
MERCAPTOPURINE
PP242
OLAPARIB
MK.2206
NVP.AEW541
NVP.BGJ398
NVP.BSK805
BUPARLISIB
BX795
SYK.INHIBITOR.IV
BMS.509744